New Journal of Physics
The open–access journal for physics

Phase mixing of shear Alfvén waves as a new mechanism for electron acceleration in collisionless, kinetic plasmas

David Tsiklauri[1,3], **Jun-Ichi Sakai**[2] **and Shinji Saito**[2]

[1] Institute for Materials Research, School of Computing, Science and Engineering, University of Salford, Gt Manchester M5 4WT, UK
[2] Laboratory for Plasma Astrophysics, Faculty of Engineering, Toyama University, 3190, Gofuku, Toyama 930-8555, Japan

New Journal of Physics **7** (2005) 79
Received 28 January 2005
Published 15 March 2005
Online at http://www.njp.org/
doi:10.1088/1367-2630/7/1/079

Abstract. Particle-in-cell (kinetic) simulations of shear Alfvén wave (AW) interaction with one-dimensional, across the uniform-magnetic field, density inhomogeneity (phase mixing) in collisionless plasma were performed for the first time. As a result, a new electron acceleration mechanism is discovered. Progressive distortion of the AW front, due to the differences in local Alfvén speed, generates electrostatic fields nearly parallel to the magnetic field, which accelerate electrons via Landau damping. Surprisingly, the amplitude decay law in the inhomogeneous regions, in the kinetic regime, is the same as in the MHD approximation described by Heyvaerts and Priest (1983 *Astron. Astrophys.* **117** 220).

Interaction of shear Alfvén waves (AWs) with plasma inhomogeneities is a topic of considerable importance both in astrophysical and laboratory plasmas. This is due to the fact, that both AWs and inhomogeneities often coexist in many of these physical systems. Shear AWs are believed to be good candidates for plasma heating, energy and momentum transport. On the one hand, in many physical situations, AWs are easily excitable and they are present in a number of astrophysical systems. On the other hand, these waves dissipate on shear viscosity as opposed to compressive fast and slow magnetosonic waves which dissipate on bulk viscosity. In astrophysical plasmas, shear viscosity is extremely small as compared to bulk viscosity. Hence, AWs are notoriously difficult to dissipate. One of the possibilities to improve AW dissipation is to introduce progressively collapsing spatial scales, $\delta l \to 0$, into the system (recall that the classical

[3] Author to whom any correspondence should be addressed.

PII: S1367-2630(05)93973-6
© IOP Publishing Ltd and Deutsche Physikalische Gesellschaft

viscous and ohmic dissipation is $\propto \delta l^{-2}$). Heyvaerts and Priest have proposed (in an astrophysical context) one such mechanism called AW phase mixing [1]. It occurs when a linearly polarized shear AW propagates in the plasma with a one-dimensional, transverse to the uniform magnetic field density inhomogeneity. In such a situation, initially, a plane AW front is progressively distorted because of different Alfvén speeds across the field. This creates progressively stronger gradients across the field (effectively in the inhomogeneous regions transverse scale collapses), and thus in the case of finite resistivity, dissipation is greatly enhanced. Thus, it is believed that phase mixing can provide substantial plasma heating. A significant amount of work has been done in the context of heating open magnetic structures in the solar corona [1]–[11]. All phase mixing studies have so far been performed in the MHD approximation; however, since the transverse scales in the AW collapse progressively to zero, MHD approximation is inevitably violated, first, when the transverse scale approaches ion gyro-radius r_i and then the electron gyro-radius r_e. Thus, we proposed to study the phase-mixing effect in the kinetic regime, i.e. we go beyond the MHD approximation. As a result, we discovered a new mechanism of electron acceleration due to wave–particle interactions which has important implications for various space and laboratory plasmas, e.g. the coronal heating problem and acceleration of solar wind.

We used 2D3V, the fully relativistic, electromagnetic, particle-in-cell (PIC) code with MPI parallelization, modified from 3D3V TRISTAN code [12]. The system size is $L_x = 5000\Delta$ and $L_y = 200\Delta$, where $\Delta(=1.0)$ is the grid size. The periodic boundary conditions for x- and y-directions are imposed on particles and fields. There are about 478 million electrons and ions in the simulation. The average number of particles per cell is 100 in the low-density regions (see below). Thermal velocity of electrons is $v_{th,e} = 0.1c$ and for ions it is $v_{th,i} = 0.025c$. The ion to electron mass ratio is $m_i/m_e = 16$. The time step is $\omega_{pe}\Delta t = 0.05$. Here, ω_{pe} is the electron plasma frequency. The Debye length is $v_{th,e}/\omega_{pe} = 1.0$. The electron skin depth is $c/\omega_{pe} = 10\Delta$, while the ion skin depth is $c/\omega_{pi} = 40\Delta$. Here ω_{pi} is the ion plasma frequency. The electron Larmor radius is $v_{th,e}/\omega_{ce} = 1.0\Delta$, while the same for ions is $v_{th,i}/\omega_{ci} = 4.0\Delta$. The external uniform magnetic field B_0 is in the x-direction and the initial electric field is zero. The ratio of electron cyclotron frequency to electron plasma frequency is $\omega_{ce}/\omega_{pe} = 1.0$, while the same for ions is $\omega_{ci}/\omega_{pi} = 0.25$. The latter ratio is essentially the Alfvén speed V_A/c. For a plasma, $\beta = 2(\omega_{pe}/\omega_{ce})^2(v_{th,e}/c)^2 = 0.02$. Here, all plasma parameters are quoted far away from the density inhomogeneity region. The dimensionless (normalized to some reference constant value of n_0) ion and electron density inhomogeneity is described by

$$n_i(y) = n_e(y) = 1 + 3\exp\{-[(y - 100\Delta)/(50\Delta)]^6\} \equiv F(y). \tag{1}$$

This means that in the central region (across y-direction), density is smoothly enhanced by a factor of 4, and there are strong density gradients of width of about 50Δ around the points $y = 51.5\Delta$ and 148.5Δ. The background temperature of ions and electrons, and their thermal velocities are varied accordingly

$$T_i(y)/T_0 = T_e(y)/T_0 = F(y)^{-1}, \tag{2}$$

$$v_{th,i}/v_{i0} = v_{th,e}/v_{e0} = F(y)^{-1/2}, \tag{3}$$

such that the thermal pressure remains constant. Since the background magnetic field along the x-coordinate is also constant, the total pressure remains constant too. Then, we impose a current

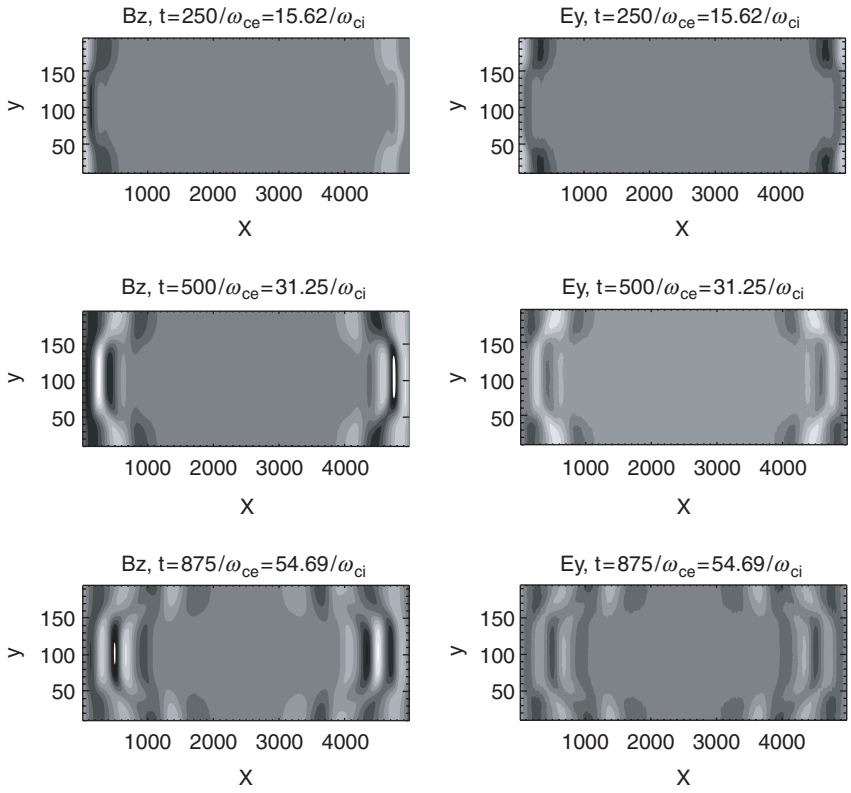

Figure 1. Contour (intensity) plots of phase mixed AW B_z and E_y components at instants: $t = (15.62, 31.25, 54.69)/\omega_{ci}$. Excitation source is at the left boundary. Because of periodic boundary conditions, left-propagating AW re-appears from the right-hand side of the simulation box. Note how AW is progressively stretched because of differences in local Alfvén speed.

of the following form:

$$\partial_t E_y = -J_0 \sin(\omega_d t)\{1 - \exp[-(t/t_0)^2]\}, \tag{4}$$

$$\partial_t E_z = -J_0 \cos(\omega_d t)\{1 - \exp[-(t/t_0)^2]\}. \tag{5}$$

Here ω_d is the driving frequency which was fixed at $\omega_d = 0.3\omega_{ci}$, which ensures that no significant ion-cyclotron damping is present. Also, ∂_t denotes a time derivative, t_0 is the onset time of the driver, which was fixed at $50/\omega_{pe}$ or $3.125/\omega_{ci}$. This means that the driver onset time is about three ion–cyclotron periods. Imposing such a current on the system results in the generation of left circularly polarized shear AW, which is driven at the left boundary of simulation box and has a width of 1Δ. The initial amplitude of the current is such that the relative AW amplitude is about 5% of the background in the low-density regions, thus the simulation is weakly non-linear.

Because no initial (perpendicular to the external magnetic field) velocity excitation was imposed in addition to the above-specified currents (cf [9]), at the left boundary, the excited (driven) circularly polarized AW is split into two circularly polarized AWs that travel in opposite directions. The dynamics of these waves is shown in figure 1, where we show three snapshots of the evolution. A typical simulation, till the last snapshot shown in the figure, takes about 8 days

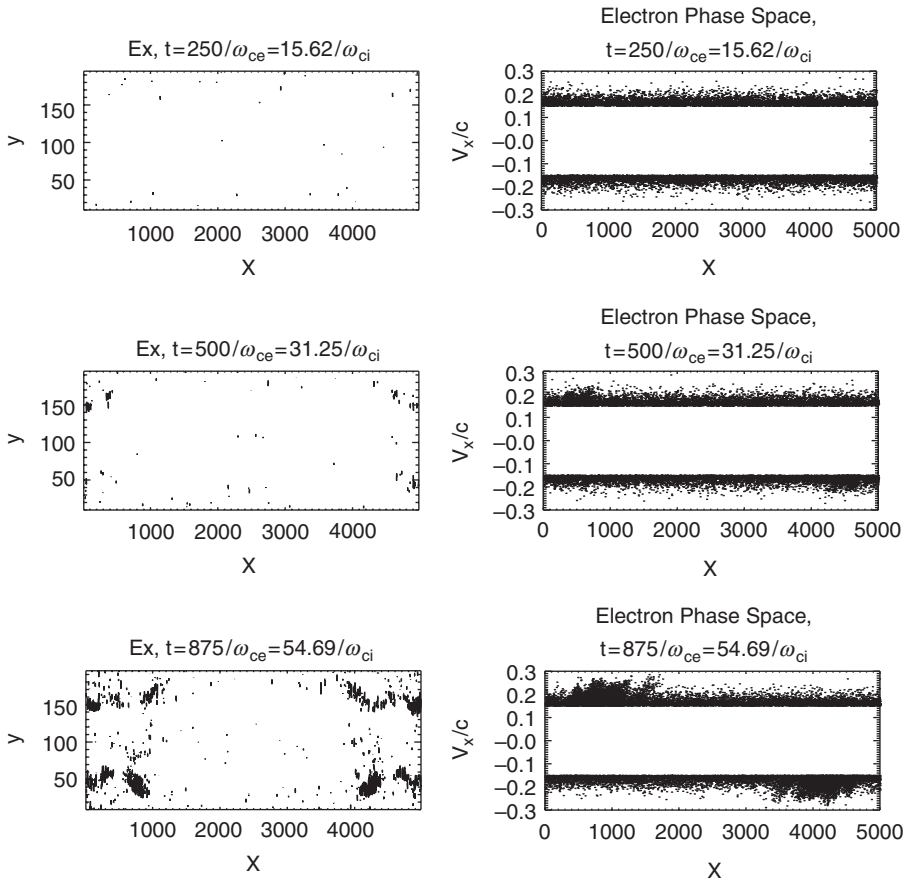

Figure 2. Left column: contour plots of electrostatic field E_x generated nearly parallel to the external magnetic field at instants: $t = (15.62, 31.25, 54.69)/\omega_{ci}$. Right column: x-component of electron phase space at the same times. Note that, in order to reduce the figure size, only electrons with $V_x > 0.15c$ were plotted.

on the parallel 32 dual 2.4 GHz Xeon processors. It can be seen from the figure that, because of the periodic boundary conditions, circularly polarized AW that was travelling to the left has reappeared from the right-hand-side of the simulation box ($t = 15.62/\omega_{ci}$). Then the dynamics of the AW (B_z, E_y) progresses in a similar manner as in MHD, i.e. it phase mixes [1]. In other words, the middle region (in y-coordinate) travels slower because of the density enhancement (note that $V_A(y) \propto 1/\sqrt{n_i(y)}$). This obviously causes distortion of the initially plane wave front and the creation of strong gradients in the regions around $y = 50$ and 150. In MHD approximation, in the case of finite resistivity η, in these regions AW is strongly dissipated due to enhanced viscous and ohmic dissipation. This effectively means that the outer and inner parts of the travelling AW are detached from each other and propagate independently. This is why the effect is called phase mixing; in the case of developed phase mixing, after a long time, phases in the wave front become effectively uncorrelated. *A priori* it was not clear what to expect from our PIC simulation because it was performed for the first time. The code is collisionless and there are no sources of dissipation in it (apart from the possibility of wave–particle interactions). It is evident from figure 1 that, at later stages ($t = 54.69/\omega_{ci}$), the AW front is strongly damped in the strong density gradient regions. This immediately raises a question: where did the AW energy go? The answer lies in figure 2, where we plot the longitudinal electrostatic field E_x, and electron phase

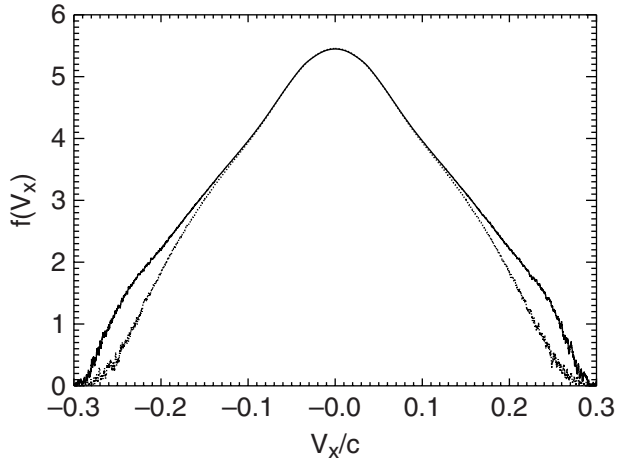

Figure 3. The distribution function of electrons at $t = 0$ (dotted curve) and $t = 54.69/\omega_{ci}$ (solid curve).

space (V_x/c versus x) for the different times (note that, in order to reduce the figure size, only electrons with $V_x > 0.15c$ were plotted). In the regions around $y = 50$ and 150, for later times significant electrostatic field is generated. This is the consequence of stretching of the AW front in those regions because of difference in the local Alfvén speed. In the right column of this figure, we see that exactly in those regions where E_x is generated, the electrons are accelerated in large numbers. Thus, we conclude that energy of the phase mixed AW goes into acceleration of electrons. In fact, line plots of E_x show that this electrostatic field is strongly damped, i.e. energy is channelled to electrons via Landau damping.

The next piece of evidence comes from looking at the distribution function of electrons before and after the phase mixing took place. In figure 3, we plot the distribution function of electrons at $t = 0$ and $54.69/\omega_{ci}$. Note that, even at $t = 0$, the distribution function does not look like a purely Maxwellian because of the fact that the temperature varies across the y-coordinate (to keep the total pressure constant) and the graph is produced for the entire simulation domain. There is also a substantial difference at $t = 54.69/\omega_{ci}$ compared to its original form because of the aforementioned electron acceleration. We see that the number of electrons having velocities $V_x = \pm(0.1 - 0.3)c$ is increased. Note that the acceleration of electrons takes place mostly along the external magnetic field (along the x-coordinate). No electron acceleration occurs in V_y or V_z (not plotted here).

The next step is to check whether the increase in electron velocities comes from the resonant wave–particle interactions. For this purpose in figure 4, we plot two snapshots of AW $B_z(x, y = 148)$ components at instances $t = 54.69/\omega_{ci}$ (solid line) and $t = 46.87/\omega_{ci}$ (dotted line). The distance between the two upper leftmost peaks (which is the distance travelled by the wave in time between the snapshots) is about $\delta L = 150\Delta = 15(c/\omega_{pe})$. Time difference between the snapshots is $\delta t = 7.82/\omega_{ci}$. Thus, the AW speed measured at the point of the strongest density gradient ($y = 148$) is $V_A^M = \delta L/\delta t = 0.12c$. Now, we can also work out the Alfvén speed. In the homogeneous low-density region, the Alfvén speed was set to be $V_A(\infty) = 0.25c$. From equation (1), it follows that, for $y = 148$, density is increased by a factor of 2.37, which means that the Alfvén speed, at this position is $V_A(148) = 0.25/\sqrt{2.37}c = 0.16c$. The measured and calculated Alfvén speeds in the inhomogeneous region do not coincide. This can be attributed to

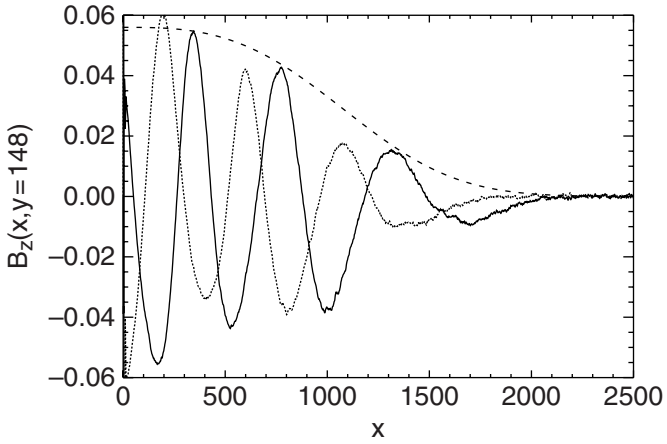

Figure 4. Two snapshots of AW $B_z(x, y = 148)$ component at instants $t = 54.69/\omega_{ci}$ (——) and $t = 46.87/\omega_{ci}$ (· · · · · ·). The dashed line represents the fit $0.056 \exp[-(x/1250)^3]$.

the fact that, in the inhomogeneous regions (where electron acceleration takes place), because of momentum conservation, the AW front is decelerated as it passes on energy and momentum to the electrons. However, this may be not the case if wave–particle interactions play the same role as dissipation in the MHD: then wave–particle interactions would result only in the decrease of the AW amplitude (dissipation), not in its deceleration. If we compare these values to figure 3, we deduce that these are the velocities $>0.12c$ above which electron numbers with higher velocities are greatly increased. This deviation peaks at about $0.25c$ which in fact corresponds to the Alfvén speed in the lower-density regions. This can be explained by the fact that the electron acceleration takes place in wide regions (cf figure 2) along and around $y = 148$ (and $y = 51$)—hence the spread in the accelerated velocities.

In figure 4, we also plot a visual fit curve (dashed line) in order to quantify the amplitude decay law for the AW (at $t = 54.69/\omega_{ci}$) in the strongest density inhomogeneity region. The fitted (dashed) curve is represented by $0.056 \exp[-(x/1250)^3]$. There is an astonishing similarity of this fit to the MHD approximation results. Hayvaerts and Priest [1] found that for large times (developed phase mixing), in the case of harmonic driver, the amplitude decay law is given by $\propto \exp[-(\frac{\eta\omega^2 V_A'^2}{6V_A^5})x^3]$ which is much faster than the usual resistivity dissipation $\propto \exp(-\eta x)$. Here V_A' is the derivative of the Alfvén speed with respect to the y-coordinate. The most intriguing fact is that, even in the kinetic approximation, the same $\propto \exp(-Ax^3)$ law holds as in the MHD. In the MHD, a finite resistivity and Alfvén speed non-uniformity are responsible for the enhanced dissipation via a phase mixing mechanism. In our PIC simulations (kinetic phase mixing), however, we do not have dissipation and collisions (dissipation). Thus, in our case wave–particle interactions play the same role as resistivity η in the MHD phase mixing. It should be noted that no significant AW dissipation was found away from the density inhomogeneity regions. This has the same explanation as in the case of MHD—it is the regions of density inhomogeneities ($V_A' \neq 0$) where the dissipation is greatly enhanced, while in the regions where $V_A' = 0$, there is no substantial dissipation (apart from the classical $\propto \exp(-\eta x)$). In the MHD approximation, the aforementioned amplitude decay law is derived from the diffusion equation, to which MHD equations reduce to for large times (developed phase mixing). It seems that the

kinetic description leads to the same type of diffusion equation. It is unclear, however, at this stage, what physical quantity would play the role of resistivity η (from the MHD approximation) in the kinetic regime.

It is worthwhile mentioning that, in the MHD approximation, [8, 11] showed that, in the case of localized Alfvén pulses, Heyvaerts and Priest's amplitude decay formula $\propto \exp(-Ax^3)$ (which is true for harmonic AWs) is replaced by the power law $B_z \propto x^{-3/2}$. A natural next step forward would be to check whether, in the case of localized Alfvén pulses, the same power law holds in the kinetic regime.

Finally, we would like to mention that, after this study was completed, we became aware of a study by [13], who used a hybrid code (electrons treated as neutralizing fluid, while ion kinetics is retained) as opposed to our (fully kinetic) PIC code, to simulate resonant absorption. They found that a planar (body) AW propagating at less than 90° to a background gradient has field lines which lose wave energy to another set of field lines by cross-field transport. Furthermore, Vasquez [14] found that when perpendicular scales of order 10 proton inertial lengths ($10c/\omega_{pi}$) develop from wave refraction in the vicinity of the resonant field lines, a non-propagating density fluctuation begins to grow to large amplitudes. This saturates by exciting highly oblique, compressive, and low-frequency waves which dissipate and heat protons. These processes lead to a faster development of small scales across the magnetic field, i.e. this is ultimately related to the phase-mixing mechanism, studied here. Continuing this argument, we would like to make a clear distinction between the effects of phase mixing and resonant absorption of the shear AWs. Historically, there was some confusion in the use of those terms. In fact, earlier studies, which were performed in the context of laboratory plasmas, e.g. [15], proposed (quote) 'the heating of collisionless plasma by utilizing a spatial phase mixing by shear AW resonance and discussed potential applications to toroidal plasma' used the term 'phase mixing' to discuss the physical effect, which in reality was the resonant absorption. In their later works, Hasegawa and Chen [16, 17], when they treated the same problem in the kinetic approximation (note that Hasegawa and Chen [15] used the MHD approach), avoided further use of the term 'phase mixing' and instead they talked about linear mode conversion of shear AW into kinetic AW near the resonance $\omega^2 = k_\parallel^2 V_A(x)$ (in their geometry, the inhomogeneity was across the x-axis). In the kinetic approximation, Hasegawa and Chen [16, 17] found a number of interesting effects including:

(i) They established that, near the resonance, initial shear AW is linearly converted into kinetic AW (which is the AW modified by the finite ion Larmor radius and electron inertia) that propagates almost parallel to the magnetic field into the higher density side. Inclusion of the finite ion Larmor radius and electron inertia removes the logarithmic singularity present in the MHD resonant absorption which exists because, in MHD, shear AW cannot propagate across the magnetic field. Physically, this means that the finite ion Larmor radius prevents tying of ions to magnetic field lines and thus allows propagation across the field. The electron inertia eliminates singularity in the same fashion but on different, $r_i\sqrt{T_e/T_i}$, spatial scale (here r_i is the ion gyro-radius).

(ii) They also found that in the collisionless regime (which is applicable to our case), dissipation of the (mode-converted) kinetic AW is through Landau damping of parallel electric fields both by electrons and ions. However, in the low plasma β regime (which is also applicable to our case, $\beta = 2(\omega_{pe}/\omega_{ce})^2(v_{th,e}/c)^2 = 0.02$) they showed that only electrons are heated

(accelerated), but not the ions. In our numerical simulations, we see a similar behaviour: i.e. preferential acceleration of electrons (cf Tsiklauri *et al* [18]). In spite of this similarity, however, one should make clear distinction between (a) phase mixing which essentially is a result of enhanced, due to plasma inhomogeneity, *collisional* viscous and ohmic dissipation and (b) resonant absorption which can operate in the *collisionless* regime as a result of generation of kinetic AW in the resonant layer, which subsequently decays via Landau damping preferentially accelerating electrons in the low β regime.

(iii) They also showed that, in the kinetic regime, the total absorption rate is approximately the same as in the MHD. Our simulations seem to produce similar results. We cannot comment quantitatively on this occasion, but at least the spatial form of the amplitude decay ($\propto \exp(-Ax^3)$) is similar in both cases.

Resuming the above discussion, we conjecture that the generated nearly parallel electrostatic fields found in our numerical simulations are due to the generation of kinetic AWs that are created through interaction of initial shear AWs with plasma density inhomogeneity, in a similar fashion as in resonant absorption described above. Further theoretical study is thus needed to provide a solid theoretical basis for interpretation of our numerical simulation results and to test the above conjecture.

Acknowledgments

The authors would like to express their particular gratitude to CAMPUS (Campaign to Promote University of Salford), which funded J-ISs one month fellowship to visit the Salford University that made this project possible. DT acknowledges the use of E Copson Math cluster funded by PPARC and University of St Andrews. DT kindly acknowledges support from Nuffield Foundation through an award to newly appointed lecturers in science, engineering and mathematics (NUF-NAL 04). DT would like to thank A W Hood (St Andrews) for encouraging discussions. We also would like to thank the referees for very useful suggestions.

References

[1] Heyvaerts J and Priest E 1983 *Astron. Astrophys.* **117** 220
[2] Nocera L, Priest E and Hollweg J 1986 *Geophys. Astrophys. Fl. Dyn.* **35** 111
[3] Parker E 1991 *Astrophys. J.* **376** 355
[4] Nakariakov V, Roberts B and Murawski K 1997 *Solar Phys.* **175** 93
[5] Moortel I D, Hood A W and Arber T 2000 *Astron. Astrophys.* **354** 334
[6] Botha G J J, Arber T D, Nakariakov V and Keenan F 2000 *Astron. Astrophys.* **363** 1186
[7] Tsiklauri D, Arber T and Nakariakov V M 2001 *Astron. Astrophys.* **379** 1098
[8] Hood A, Brooks S and Wright A N 2002 *Proc. R. Soc.* A **458** 2307
[9] Tsiklauri D and Nakariakov V M 2002 *Astron. Astrophys.* **393** 321
[10] Tsiklauri D, Nakariakov V M and Arber T 2002 *Astron. Astrophys.* **395** 285
[11] Tsiklauri D, Nakariakov V M and Rowlands G 2003 *Astron. Astrophys.* **400** 1051
[12] Buneman O 1993 *Computer Space Plasma Physics Simulation Techniques and Software* (New York: Terra Scientific) p 67
[13] Vasquez B J and Hollweg J V 2004 *Geophys. Res. Lett.* **31** L14803

[14] Vasquez B J 2004 *J. Geophys. Res.* submitted
[15] Hasegawa A and Chen L 1974 *Phys. Rev. Lett.* **32** 454
[16] Hasegawa A and Chen L 1975 *Phys. Rev. Lett.* **35** 370
[17] Hasegawa A and Chen L 1976 *Phys. Fluids.* **19** 1924
[18] Tsiklauri D, Sakai J I and Saito S 2005 *Astron. Astrophys.* at press